

AN AUGMENTED SPACE RECURSION STUDY OF THE ELECTRONIC STRUCTURE OF ROUGH EPITAXIAL OVERLAYERS

Biplab Sanyal, Parthapratim Biswas, A. Mookerjee

S.N. Bose National Centre for Basic Sciences

JD Block, Sector 3, Salt Lake City, Calcutta 700091, INDIA

Hemant G Salunke and G.P. Das

Bhabha Atomic Research Centre, Trombay, Mumbai , INDIA

and

A.K. Bhattacharyya

Centre for Catalysis and Materials Studies,

Department of Engineering, University of Warwick, Coventry, England

October 13, 2018

Abstract

In this communication we propose the use of the Augmented Space Recursion as an ideal methodology for the study of electronic and magnetic structures of rough surfaces, interfaces and overlayers. The method can take into account roughness, short-ranged clustering effects, surface dilatation and interdiffusion. We illustrate our method by an application of Fe overlayer on Ag (100) surface.

1 Introduction

Magnetism at surfaces, overlayers and interfaces has evoked much interest in recent times [1]. The chemical environment of an atom at a surface or overlayer is very different from the bulk. The difference in environment, existence of surface states and hybridization of the states of the overlayer with those of the substrate can give rise to a wide variety of new and interesting material and magnetic properties. This wide variety has the potential for being the basis of surface materials design. This is the underlying reason for the absorbing theoretical interest in this field.

In this communication we wish to argue that the Augmented Space Recursion (ASR) introduced by us earlier is one of the most suitable techniques for the study of rough overlayers and interfaces.

First principles all electron techniques for the determination of the electronic structure based on the local spin density approximation (LSDA) have made reasonably accurate quantitative calculations possible. Originally the most popular of the methods was the parametrized tight-binding or the linear combination of atomic orbitals (LCAO) method [2]. However, the fact that the parametrized hamiltonian is, in general, never transferable and that the basis does not have sufficient variational freedom, has led to the eclipse of such methods for quantitative calculations ; in particular of properties as sensitive to these assumptions as the magnetic moment . There have been attempts of resuscitating the LCAO by introducing ideas of environment dependent parametrization [3] . The generally accepted quantitative techniques include the Augmented Plane Wave (APW) and its linearized version (LAPW)[4] and the Korringa-Kohn-Rostocker (KKR) and its linearized version (LMTO)[5]. The two basically related methods come both in the Full Potential versions where no assumption is made about the shape of the charge density

or the potential, or in the spherically symmetrized Muffin-tin Potential versions. The electrons may be treated either semi-relativistically or fully relativistically [6]. In addition, Andersen and co-workers [7] have proposed a tight-binding LMTO (TB-LMTO) where the real space representation of the hamiltonian is sparse. Which of the two basic methods we choose often depends on a matter of taste and history. Moreover, how far we wish to go down the ladder of different approximations is guided by the accuracy required and the computational heaviness we wish to face. We would not like to comment on this, other than justifying the specific technique we have chosen for ourselves.

The other important aspect of the problem is the loss of translational symmetry perpendicular to the surface. This aspect has been dealt with by different authors in different ways :

- (i) finite slab calculations, which assume that finite size effects are negligible [8]
- (ii) supercell calculations, where the translational symmetry is restored. Each supercell has a replica of the finite system and the assumption is that the supercells are large enough so as not to affect one another
- (iii) the slab Green function method where the translational symmetry parallel to the surface is utilized and the perpendicular direction is treated in real space [9]-[11]. The embedding method of Inglesfield and coworkers [12] belongs to this group, where the Green function of the semi-infinite solid is calculated by downfolding onto this semi-infinite subspace.
- (iv) the fully real space based Recursion method [13] which does not require any translational symmetry and was originally developed for dealing with surfaces and interfaces.

Overlays produced by molecular beam epitaxy and other vapor deposition techniques are, by and large, rough. Local probes, such as STM techniques, reveal steps, islands and pyramid-like structures. Moreover, there is always interdiffusion between the overlayer and the substrate leading to a disordered alloy like layer at the interface. This brings in the last important aspect of the problem : roughness or disorder parallel to the surface. A majority of the theoretical work done on surfaces and overlays so far had always assumed flat layers. These generally involve the use of surface Green functions, $G(k_{\parallel},z)$, which allow breaking of translational symmetry perpendicular to the surface, but presume such symmetry parallel to it [9, 10]. Roughness has been introduced in overlays by randomly alloying it with *empty spheres* [11]. Such alloying has been assumed to be homogeneous and has been treated within a mean field or the coherent potential approximation (CPA) . Attempts at going beyond the CPA has not been generally successful. One of the more successful approaches in this direction is the Augmented Space Formalism (ASF)[14] and techniques basically based on it, like the travelling cluster approximation (TCA) [15].

Let us now justify why we wish to introduce the Augmented Space Recursion based on the TB-LMTO as an attractive method for the study of rough surfaces, overlays or interfaces.

The CPA has proven to be an accurate approximation in a very large body of applications. Why then do we wish to go beyond ? We should recall that the CPA is exact when the local coordination is infinite. Its accuracy is inversely proportional to the local coordination. We therefore expect the CPA to be comparatively less accurate at a surface as compared with the bulk calculations. Further, the CPA basically describes homogeneous randomness. It cannot accurately take into account clustering, short-ranged ordering or local lattice distortions, of the kind we expect to encounter in the rough surfaces produced experimentally. The ASF allows us to describe exactly such situations, without violating

the so called “herglotz” properties which the approximated averaged Green function must possess [16].

We shall combine the ASF with the Recursion method to calculate the configuration averaged Green functions. We should note that the Augmented Space Theorem is exact [16] and the approximation involves in terminating the recursion-generated continued fraction. Analyticity preserving “terminators” have been introduced by Haydock and Nex [17] and Lucini and Nex [18]. Recently Ghosh *et.al.* [19] have discussed the convergence of the Augmented Space Recursion and indicated how to generate physical quantities within a prescribed error window. The Recursion method, being entirely in real space, does not require any translational symmetry and is ideally suited for systems with inhomogeneous disorder. However, for the Recursion method to be a practicable computational technique, we must choose a basis of representation in which the effective hamiltonian is sparse, i.e. short ranged in real space. The best choice of a computationally simple yet accurate basis is the TB-LMTO. This is what we describe in this communication. However, the screened-KKR [6] would also be a more quantitatively accurate choice. We would require the energy dependent extension of the Recursion method. This has been developed recently [20] and its application to the screened-KKR will be described in a subsequent communication.

To illustrate the method we shall take a well studied example : that of Fe deposited on the (100) surface of a Ag substrate. The lattice parameter of bcc Fe, the most commonly known ferromagnet [21] matches the nearest neighbour distance on the (100) surface of fcc Ag (half the face diagonal), a very good non magnetic electrical conductor. This favours epitaxial deposition of bcc Fe on Ag(100) manifesting interesting magnetic properties.

Before describing the methodology in some detail we need to clarify the following point : in order to describe inhomogeneous disorder we have taken recourse to the Gener-

alized Augmented Space Theorem [22]. This generalized ASF does take into account short-ranged order through the Warren-Cowley parameter and yields an analytic herglotz approximation. In a recent publication [23] the authors make the strange statement that the generalized ASF yields negative densities of states and quotes the work of Razee and Prasad [24]. The statement is untrue and the misconception should be cleared up. A careful reading of the quoted article [24] will show that in applying the generalized ASF Razee and Prasad use the Nikodym-Radon transform and write the joint density of states of the hamiltonian parameters $\mathcal{P}(\{\epsilon_i\})$ as $(\prod p(\epsilon_i)) \Phi(\{\epsilon_i\})$. For homogeneous disorder $\Phi(\{\epsilon_i\})$ is unity, while for inhomogeneous disorder the authors expand the function as an infinite series involving various correlation functions between the $\{\epsilon_i\}$ (the simplest two site correlation can be written in terms of the Warren-Cowley parameter). They then truncate this series after a few terms. This extra approximation cannot guarantee the preservation of the herglotz analytic properties and is the cause of the observed negative density of states in some energy regimes. The generalized ASF described by Mookerjee and Prasad [22] does not take recourse to such an approximation and has been shown to be exact in the referenced paper. Approximation then arises entirely due to the recursion termination - which has been shown to preserve the herglotz analytic properties.

2 The Generalized Augmented Space Theorem

In this section we shall describe the generalized Augmented Space Formalism. The hamiltonian is a function of a set of random variables $\{n_i\}$ which are not independent, so that the joint probability distribution can be written in terms of the conditional probability densities of the individual variables as :

$$p(\{n_i\}) = p(n_1) \prod_k p(n_k | n_{k-1}, n_{k-2}, \dots, n_1)$$

Each random variable n_k has associated with it its own configuration space Φ_k and, in the case of correlated disorder, a set of operators $\{M_k^{\lambda_{k-1}, \lambda_{k-2}, \dots, \lambda_1}\}$ whose spectral density are the conditional probability densities of the random variable, dependent on the configurations of the previous labeled ones. The λ_k label the configurations of the variable n_k . The configuration space of the set of random variables is the product $\Psi = \prod_k^\otimes \Phi_k$. What the generalized augmented space theorem proved was that, if we define operators on this full configuration space,

$$\tilde{M}_k = \sum_{\lambda_1} \sum_{\lambda_2} \dots \sum_{\lambda_{k-1}} P_1^{\lambda_1} \otimes P_2^{\lambda_2} \otimes \dots P_{k-1}^{\lambda_{k-1}} \otimes M_k^{\lambda_{k-1}, \lambda_{k-2}, \dots, \lambda_1} \otimes I \otimes I \dots$$

then the configuration average of any function of the hamiltonian is given exactly by :

$$\langle\langle \mathcal{F}(\{n_k\}) \rangle\rangle = \langle F^0 | \tilde{\mathcal{F}}(\{\tilde{M}_k\}) | F^0 \rangle \quad (1)$$

The average state $|F^0\rangle$ is defined by :

$$\begin{aligned} |F^0\rangle &= \prod_k |f_k^0\rangle \\ |f_k^0\rangle &= \sum_{\lambda_k} \sqrt{\omega_{\lambda_k}^{\lambda_1, \lambda_2, \dots, \lambda_{k-1}}} |\lambda_k\rangle \end{aligned}$$

where the numbers under the root sign are the conditional probability weights for the various configurations of the variable n_k .

In our model, the random variables are the occupation variables of a site by two different kind of atoms . The simplest model is one that assumes that the occupation of the nearest

neighbours of a site depends on its own occupation. The probability densities are given by :

$$\begin{aligned}
 p(n_1) &= x \delta(n_1 - 1) + y \delta(n_1) \\
 p(n_2|n_1 = 1) &= (x + \alpha y) \delta(n_2 - 1) + (1 - \alpha) y \delta(n_2) \\
 p(n_2|n_1 = 0) &= (1 - \alpha) x \delta(n_2 - 1) + (y + \alpha x) \delta(n_2)
 \end{aligned}$$

Where x and y are the concentrations of the constituents and α is the Warren-Cowley short-ranged order parameter. $\alpha=0$ refers to the completely random case, when the various operators $M_k^{\lambda_{k-1}, \dots, \lambda_1}$ become independent of the superscripts and the generalized augmented space theorem reduced to the usual augmented space theorem. $\alpha < 0$ indicates tendency towards ordering alternately, while $\alpha > 0$ indicates tendency towards segregation.

The representations of the corresponding operators required are the following :

$$\begin{aligned}
 M_1 &= \begin{pmatrix} x & \sqrt{xy} \\ \sqrt{xy} & y \end{pmatrix} \\
 M_2^1 &= \begin{pmatrix} x + \alpha y & \sqrt{(1 - \alpha)y(x + \alpha y)} \\ \sqrt{(1 - \alpha)y(x + \alpha y)} & (1 - \alpha)y \end{pmatrix} \\
 M_2^0 &= \begin{pmatrix} (1 - \alpha)x & \sqrt{(1 - \alpha)x(y + \alpha x)} \\ \sqrt{(1 - \alpha)x(y + \alpha x)} & y + \alpha x \end{pmatrix}
 \end{aligned}$$

$$P_1^0 = \begin{pmatrix} x & \sqrt{xy} \\ \sqrt{xy} & y \end{pmatrix}$$

$$P_1^1 = \begin{pmatrix} y & -\sqrt{xy} \\ -\sqrt{xy} & x \end{pmatrix}$$

3 TB-LMTO-ASR formulation

Our system consists of a semi-infinite Ag substrate with layers of Fe atoms on the (100) surface. We shall describe the hamiltonian of the electrons within a tight- binding linearized muffin-tin orbitals basis (TB-LMTO). As described earlier, we shall take care of the charge leakage into the vacuum by layers of empty spheres containing charge but no atoms. We shall roughen the topmost layer by randomly alloying the Fe atoms with empty spheres. We shall allow for short-ranged order in the alloying. Segregation will imply that the Fe atoms and empty spheres cluster together forming islands and clumps. Ordering on the other hand will imply that Fe atoms like to be surrounded by empty spheres and vice versa.

The details of the description of the effective augmented space hamiltonian has been described at length in an earlier paper [25]. We shall indicate the generalization of that result when nearest neighbour short-ranged order is introduced as described above.

$$\begin{aligned} \tilde{H} = & \mathbf{H}_1 \tilde{\mathbf{I}} + \mathbf{H}_2 \sum_k \mathbf{P}_k \otimes \mathbf{P}_\downarrow^k + \mathbf{H}_3 \sum_k \mathbf{P}_k \otimes \{\mathbf{T}_{\downarrow\uparrow}^k + \mathbf{T}_{\uparrow\downarrow}^k\} \\ & + \mathbf{H}_4 \sum_k \sum_{k'} \mathbf{T}_{kk'} \otimes \mathbf{I} + \alpha \mathbf{H}_2 \sum_{m \in N_1} \mathbf{P}_m \otimes \mathbf{P}_\downarrow^1 \otimes \{\mathbf{P}_\uparrow^m - \mathbf{P}_\downarrow^m\} + \end{aligned}$$

$$\begin{aligned}
& + \mathbf{H}_5 \sum_{m \in N_1} \mathbf{P}_m \otimes \mathbf{P}_\uparrow^1 \otimes \{\mathbf{T}_{\uparrow\downarrow}^m + \mathbf{T}_{\downarrow\uparrow}^m\} + + \mathbf{H}_6 \sum_{m \in N_1} \mathbf{P}_m \otimes \mathbf{P}_\downarrow^1 \otimes \{\mathbf{T}_{\uparrow\downarrow}^m + \mathbf{T}_{\downarrow\uparrow}^m\} + \\
& + \alpha \mathbf{H}_2 \sum_{m \in N_1} \mathbf{P}_m \otimes \{\mathbf{T}_{\uparrow\downarrow}^1 + \mathbf{T}_{\downarrow\uparrow}^1\} \otimes \{\mathbf{P}_\uparrow^m - \mathbf{P}_\downarrow^m\} + \\
& + \mathbf{H}_7 \sum_{m \in N_1} \mathbf{P}_m \otimes \{\mathbf{T}_{\uparrow\downarrow}^1 + \mathbf{T}_{\downarrow\uparrow}^1\} \otimes \{\mathbf{T}_{\uparrow\downarrow}^2 + \mathbf{T}_{\downarrow\uparrow}^2\}
\end{aligned} \tag{2}$$

where, N_1 are the set of nearest neighbours of the site labeled 1 on the surface and for calculations of averaged local densities of states at a constituent labeled by λ we have

$$\begin{aligned}
\mathbf{H}_1 &= A(C/\Delta)\Delta_\lambda - (E A(1/\Delta)\Delta_\lambda - 1) \\
\mathbf{H}_2 &= B(C/\Delta)\Delta_\lambda - E B(1/\Delta)\Delta_\lambda \\
\mathbf{H}_3 &= F(C/\Delta)\Delta_\lambda - E F(1/\Delta)\Delta_\lambda \\
\mathbf{H}_4 &= (\Delta_\lambda)^{-1/2} S_{RR'} (\Delta_\lambda)^{-1/2} \\
\mathbf{H}_5 &= F(C/\Delta)\Delta_\lambda \left[\sqrt{(1-\alpha)x(x+\alpha y)} + \sqrt{(1-\alpha)y(y+\alpha x)} - 1 \right] \\
\mathbf{H}_6 &= F(C/\Delta)\Delta_\lambda \left[y\sqrt{(1-\alpha)(x+\alpha y)/x} + x\sqrt{(1-\alpha)(y+\alpha x)/y} - 1 \right] \\
\mathbf{H}_7 &= F(C\Delta)\Delta_\lambda \left[\sqrt{(1-\alpha)y(x+\alpha y)} - \sqrt{(1-\alpha)x(y+\alpha x)} \right]
\end{aligned} \tag{3}$$

$$\begin{aligned}
A(Z) &= x Z_A + y Z_B \\
B(Z) &= (y - x) (Z_A - Z_B) \\
F(Z) &= \sqrt{xy} (Z_A - Z_B)
\end{aligned}$$

The C , Δ and S are matrices in angular momenta, the first two being diagonal. We note first of all that when the short-ranged order disappears and $\alpha = 0$, the terms \mathbf{H}_5 to \mathbf{H}_7 also becomes zero and the hamiltonian reduces to the standard one described earlier [25].

This effective hamiltonian is sparse in the TB-LMTO basis, but as the expressions show there is an energy dependence in the first three terms. This compels us to carry out recursion at every energy step. However, Ghosh et. al. [20] have shown that the corresponding energy dependence of the continued fraction coefficients is very weak and if we carry out recursions at a few selected seed energies across the spectrum, we may obtain accurate results by spline fitting the coefficients over the spectrum.

For the self-consistent calculations we require to calculate the partial (atom projected) density of states at various sites in different layers. This is done by running the recursion starting from sites in different layers. We shall assume that after 5 layers from the surface bulk values are obtained. We checked that this is indeed the case, by comparing the results for the 5-th layer and a full bulk calculation. The Fermi-energy of the system is that of the bulk substrate which we have taken from the bulk calculations. In all cases we have used upto seven shells in augmented space and terminated the recursion after 8-10 steps of recursion. We have used the terminator proposed by Lucini and Nex [18]. As discussed in an earlier paper [19] , we have made sure that the moments of the densities of states converges with the number of augmented space shells and recursions within a preassigned error range, which is consistent with the errors made in the TB-LMTO approximations. We have made the recursive calculations LDA self-consistent. For this we had to obtain the radial solutions of the Schödinger equation involving the spherically symmetric LDA potential

$$V_p^\lambda(r) = -2\frac{Z^\lambda}{r} + V_p^{\lambda,H}[\rho^\lambda(r)] + V_p^{\lambda,XC}[\rho^\lambda(r)] + \sum_L \sum_q M_{pq}^L Q_q^L$$

λ labels the type of atom, Z^λ its atomic number, p labels the particular layer. The second term in the equation is the Hartree potential, which is obtained by solving the Poisson equation with the layer and atom projected charge densities. The third term is the exchange-correlation term. For this term we have used the Barth-Hedin form. In the last term

$$Q_p^L = \sum_{\lambda} x_p^{\lambda} \left\{ \frac{\sqrt{4\pi}}{2\ell+1} \int_0^s Y_L(\hat{r}) |r|^{\ell} \rho_p^{\lambda}(r) dr - Z^{\lambda} \delta_{\ell,0} \right\}$$

Here λ for the overlayer is either Fe or empty sphere and the concentrations x_p^{λ} is either x or $(1-x)$. For the substrate λ refers only to Ag and its concentration is 1, while for the charge layers outside the overlayer λ refers to the empty sphere and its concentration is also 1.

This last term describes the effect of redistribution of charge near the surface which is particularly important for surface electronic structure. This charge density near the surface is far from spherically symmetric. We have taken both the monopole ($\ell=0, m=0$) and the dipole ($\ell=1, m=0$) contributions. We have also averaged the multipole moments in each layer and used the technique described by Skriver and Rosengaard [26] to evaluate the matrices M_{pq}^L by an Ewald technique.

4 Results and Discussion.

In order to compare our results with calculations carried out earlier, we shall first carry out calculations on a (100) surface of bcc Fe. Earlier Wang and Freeman [2] had used the LCAO method for the study of the same system. The FP-LAPW had been used by Ohnishi *et.al.* [4] also the study the (100) surface of bcc Fe. The bulk lattice parameter was chosen (as in the case of Ohnishi *et.al.*) to be 5.4169 a.u. At this stage no lattice

relaxation was considered. The results quoted below were for the semi-relativistic self-consistent LSDA TB-LMTO both supercell and ASR. The following table compares the magnetic moment per atom for the three different methods quoted above :

	S	S-1	S-2	B
Wang and Freeman	3.01	1.69	2.13	2.16
Ohnishi <i>et.al.</i>	2.98	2.35	2.39	2.25
Sanyal <i>et.al.</i> ^(a)	2.86	2.16	2.38	2.17
Sanyal <i>et.al.</i> ^(b)	2.99	2.17	2.38	2.27

Table 1 Magnetic moments in bohr-magneton/atom

^(a) supercell and ^(b) ASR calculations

Our central layer magnetic moment per atom is close to the bulk value given by Wang and Freeman and slightly lower than that given by Ohnishi *et.al.*. All three methods exhibit Friedel oscillations in the magnetic moment, although Wang and Freeman's oscillations are larger than both Ohnishi *et.al.* and our work. Our magnetic moment at the surface layer is rather small as compared to the earlier works. However, in these initial calculations (shown as (a) in the table) we have not taken into account surface relaxation. Local lattice relaxation can be easily taken into account within the TB-LMTO-ASR [27]. We refer the reader to the details of the relaxation method in the reference mentioned. A 7-8 % relaxation of the surface layer leads to a surface magnetic moment of $2.99 \mu_B/atom$ which is in good agreement with both the earlier works (shown as (b) in Table 1).

We shall now turn to the study of Fe (100) on the (100) surface of fcc Ag substrate. We shall carry out the calculations using two different techniques. First, we shall use the Tight Binding Linearised Muffin Tin Orbital (TB-LMTO) method with a minimal (s,p,d) basis set for Fe and Ag sites in a tetragonal supercell. Both spin polarized as well as non-spin polarized calculations were performed on a Fe/Ag multilayer containing a monolayer of Fe, a monolayer of empty spheres above them and four Ag layers as the substrate. The empty spheres take care of the charge leakage into the vacuum across the free surface.

The results of the calculation show that spin polarization yields a lower total ground state energy as compared with the unpolarised case by ~ 0.092 eV/atom suggesting that the ground state is magnetic. All the Fe layers have ferromagnetically arranged moments with interface Fe layers having a magnetic moment of $\sim 2.86\mu_B$ (bulk value $2.27\mu_B$). Also Fe induces a ferromagnetic moment in Ag at the interface of $\sim 0.012\mu_B$ per atom. The calculation also suggests Friedel oscillations in net valence charge in Ag as one goes from interface to bulk in Ag. This is because of moment spillage into the empty spheres. Such moment spillage outside the surface has also been observed by Ohnishi *et.al.* [4].

We shall refine our calculations in three steps. First we shall introduce the local lattice relaxation technique within the TB-LMTO-ASR [27] to relax the surface layer. We shall inflate the interlayer distance between the surface layer and the one just below it. Figure 1 shows the variation of the magnetic moment at the surface layer as a function of the percentage lattice dilatation at the surface. The minimum of the total energy occurs at around 7.5% dilatation. Here the moment carried by the monolayer of Fe is $3.17\mu_B/atom$, which is not very far from the value of $3.1\mu_B/atom$ quoted by Blügel based on FP-LAPW calculations [28].

Next we shall begin with a planar monolayer of Fe on Ag and roughen the monolayer by alloying it with empty spheres. We shall now use the self-consistent ASR for obtaining the electronic density of states and local magnetization as a function of the concentration of alloying and the short-range order parameter. We shall begin the LDA-self-consistency by using, to start with, the converged potential parameters from the supercell calculations on planar surfaces and the equilibrium lattice distances i.e. with a 7.5 % surface lattice dilatation. With this starting point the self-consistency is reached much faster than otherwise.

Figure 2(a) shows the local density of states at a point in the bulk Ag substrate (full lines) and that for an Ag atom on the 100 surface of fcc Ag (without the deposited Fe overlayer) (dotted lines), obtained by a eight-step recursion process. We have checked that the recursion does converge in the sense suggested by Haydock [13] and Ghosh *et.al.* [19] of the convergence of integrals of the form

$$\int_{-\infty}^E \Phi(E') n(E') dE'$$

where $\Phi(E)$ is a well-behaved, monotonic function in the integration range. The Fermi-energy or the chemical potential is calculated from the bulk and is shown in the Figure 2(a). As expected we notice that the d-band width decreases at the surface. This is expected, as the surface atoms are less coordinated than the bulk (eight on the 100 surface as against twelve in the bulk). There is also a redistribution of spectral weight in the band. It is clear that the amount of charge in a Wigner-Seitz sphere around a surface atom is less than that around a bulk atom. This extra charge leaks out into the so-called empty-spheres, which carry no atoms but only this leaked charge. By the time we go down about four layers below the surface, we begin to get local densities indistinguishable from the bulk results.

Figure 2(b) Shows the local density of states for the up and down electrons in the Fe overlayer. This is for a perfectly planar overlayer on the 100 surface. As is usual in either bulk Fe or Fe overlayers on noble metals, the majority occupied spin band (here up) shows much more structure than the minority occupied one (here down). Since the Ag d-bands centered round -0.5 ryd do not overlap with either of the Fe d-bands around -0.2 ryd and -0.1 ryd, there is no significant hybridization of these two, which usually leads to a widening of the Fe d-bands and consequent lowering of the local magnetic moment. The Fermi-energy is that of the bulk Ag and is shown in the figure.

We now alloy the overlayer with empty spheres and re-converge the self-consistent ASR. In Figure 3 we show the local magnetic moment on a Fe atom in the rough overlayer as a function of the Fe concentration in that layer (dotted line) with 7.5 % surface dilatation. For concentration $x=1$ of Fe we obtain the local magnetic moment corresponding to that of Figure 2(b). The value of $3.17 \mu_B/atom$ is a considerable enhancement on bulk bcc iron local magnetic moment. The agreement with the supercell calculations is very close. Blügel has argued [28] that this can be inferred from the Stoner criterion because of the narrowing of the overlayer d-bands as compared with the bulk. As we alloy the overlayer with empty spheres, the local magnetic moment on an Fe atom increases, until in the extreme case it approaches that of an isolated Fe atom at $> 3.6 \mu_B/atom$. Again we much understand this from Blügel's argument. We find that the empty spheres hardly inherit any induced magnetization, as a result as the concentration of empty spheres increase, the average coordination of Fe atoms decrease, thus increasing the magnetic moment. In the extreme limit we obtain the case of an Fe impurity atom sitting in a sea of empty spheres. Its magnetic moment approaches that of a free Fe atom. The only difference is caused by its hybridization with the Ag substrate. Figure 3 also shows (full lines) the averaged magnetization in the overlayer. This is defined by : $x M_{Fe} + y M_{ES}$. Since M_{ES} is negligible, this average overlayer magnetization decreases almost linearly with x and vanishes at $x=0$. The two types of magnetization shown in the figure are measured by local magnetic probes and global magnetization experiments.

Figure 4 shows the local magnetization at atoms in different layers . We clearly see that there is an induced magnetization in the Ag atoms of the topmost substrate layers. Magnetization oscillates layer wise into the bulk.

Figure 5 shows the variation of the local magnetic moment at a Fe site (dotted line) and the averaged magnetic moment in the overlayer as a function of the Warren-Cowley

short-ranged order parameter for (a) $x=0.9$ and (b) $x= 0.75$. We note that when the Warren-Cowley parameter indicates phase segregation the magnetic moment shows an increase. We may understand this behaviour from the following argument :

For $\alpha > 0$ the tendency is towards phase segregation. Islands of Fe (in our case, clusters of nearest neighbour atoms) precipitate in a sea of empty spheres (particularly in the low Fe concentration regime). This situation mimics the islands and pyramids observed in actual MBE deposited surfaces. A simple calculation with an isolated five atom nearest neighbour cluster sitting on the surface shows that the local density of states on the cluster is much narrower than a homogeneous distribution of Fe atoms on the surface. This leads to a larger magnetic moment/atom on the cluster. The maximum enhancement of the magnetic moment due to short-ranged clustering is around 3 %.

Clustering enhancement of magnetic moment competes with the ‘poisoning’ effect. Interfaces are never sharp, there is always an interdiffusion of substrate atoms into the surface layer and vice versa. In our final calculation we have taken a perfectly planar (non rough) monolayer of Fe on the (100) surface of fcc Ag and allowed upto 10% interdiffusion of Fe and Ag atoms in the surface layer and the one just below it. The surface layer is then an alloy Fe_xAg_{1-x} and the next layer an alloy Ag_xFe_{1-x} . The following table shows the magnetic moments in the surface layer for different values of x.

x	Averaged Mag. Mom.	Fe Mag. Mom.	Ag Mag. Mom.
0.95	3.02	3.18	0.014
0.90	2.86	3.17	0.017

Table 2 Lowering of Surface magnetism due to ‘poisoning’ by substrate

All magnetic moments are in ($\mu_B/atom$)

We notice that the depletion of magnetic moment due to poisoning by the substrate is about 4.5%. In an actual experimental situation both the enhancement effects due to sur-

face lattice dilatation and clustering and the depletion effect due to poisoning are present simultaneously. We have a handle on the determination of the lattice dilatation. Surface roughness may be probed with local techniques like the STM . If we could determine the amount of interdiffusion, we would be in a position to quantitatively predict the surface magnetic moment. The conclusion of this communication is to suggest that the Augmented Space Recursion coupled with any first principles and accurate technique which yields a sparse hamiltonian representation (like the TB-LMTO or the screened KKR) can take into account surface roughness, short-ranged clustering, surface dilatation and interdiffusion effects accurately and it would be an useful methodology to adopt.

ACKNOWLEDGEMENTS

A.M., G.P.D. and B.S. should like to thank the ICTP and its Network Project and the DST, India for financial support of this work. P.B. would like to thank the C.S.I.R., India for its financial assistance. The collaborative project between the University of Warwick and the S.N.Bose National Centre is also gratefully acknowledged. We should like to thank I. Dasgupta and T. Saha-Dasgupta whose bulk LDA-self- consistent codes formed the basis of this surface generalization.

FIGURE CAPTIONS

Figure 1 Surface magnetic moment (bohr-magneton/atom) as a function of % surface dilatation (dilatation of the distance between the surface overlayer and the next layer in the substrate)

Figure 2

(a) Local density of states at a Ag atom in the bulk (dotted line) and on the (100) surface (full lines)

(b) Local density of states at a Fe atom in an overlayer on the (100) surface of a Ag substrate. Both the up spin and the down spin densities are shown.

Figure 3 Local magnetic moment (dotted line) and averaged magnetic moment (full line) on a Fe atom in a rough overlayer on the (100) surface of a Ag substrate. Roughness is modelled by an alloy of Fe and empty spheres. The magnetic moments are shown as a function of the concentration of Fe in this model alloy. Results are for 7.5% surface dilatation.

Figure 4 Oscillation of magnetic moment on different layers of a Fe overlayer on the (100) surface of a Ag substrate.

Figure 5 Surface magnetic moment (bohr-magneton/atom) as a function of the Warren-Cowley short-ranged order parameter for (a) 90% Fe 10% Empty spheres and (b) 75% Fe 25% Empty spheres in the surface overlayer with 7.5% surface dilatation.

References

- [1] *Polarized Electrons in Surface Physics*, edited by Feder R., (World Scientific, Singapore) (1985)
- [2] Tersoff J. and Falicov L.M., Phys.Rev. **B24** 754 (1981) ; Victoria R.H., Falicov L.M. and Ishida S., Phys.Rev. **B30** 3896 (1984); Pastor G.M., Dorantes-Davila J. and Bennemann K., Phys.Rev. **B40** 7642 (1989); Riedinger R., Habar M., Stauffer L., Dreyssse H., Leonard P. and Mukherjee M., Phys.Rev. **B39** 13175 (1989); Dorantes-Davila J., Vega A. and Pastor G., Phys.Rev. **B47** 12995 (1993); Wang C.S. and Freeman A.J., Phys.Rev. **B24** 4364(1981)
- [3] Fabricius G., Llois A.M., Weissman M. and Khan M.A., Phys.Rev. **B49** 2121 (1994)
- [4] Wimmer E., Krakauer H., Weinert M. and Freeman A.J., Phys.Rev. **B24** 864 (1981) ; Ohnishi S., Freeman A.J. and Weinert W., J. Magn. Magn. Mater. **31-34** 889 (1983), Phys.Rev. **B28** 6741 (1983); Phys.Rev. **B30** 36 (1984)
- [5] Skriver H.L., *The LMTO Method* (Springer-Verlag, Berlin, 19984) ; Peduto P.R., Frota-Pessoa S. and Methfessel M.S., Phys.Rev. **B44** 13283 (1991) ; Khan M.A., Appl. Surf. Sci. **65** 18 (1993), J. Phys. Soc. Jpn. **62** 1682(1993)
- [6] Szunyogh L., Újfalussy B. and Weinberger P., Phys.Rev. **B55** 14392 (1997) (and references therein)
- [7] Andersen O.K., Jepsen O. and Gloetzel D., *Highlights of Condensed Matter Theory* , ed. Bassani F., Fumi F. and Tosi M. (North-Holland, Amsterdam, 1985); Andersen O.K., Jepsen O. and Šob M., *Electronic Structure of Metals and Alloys*, ed. Andersen O.K., Kumar V. and Mookerjee A. (World Scientific, Singapore, 1991)
- [8] Callaway J. and Wang C.S., Phys.Rev. **B16** 1095 (1977)

[9] Kudrnovský J., Wenzien B., Drchal V. and Weinberger P., Phys. Rev. **B44** 4068 (1991)

[10] Kudrnovský J., Turek I., Drchal V., Weinberger P., Christensen N.E. and Bose S.K., Phys. Rev. **B46** 4222 (1992)

[11] Ganduglia-Pirovano M.V., Kudrnovský J., Turek I., Drchal V. and Cohen M.H., Phys. Rev. **B48** 1870 (1993)

[12] Inglesfield J.E., J. Phys. **C4** L14 (1971); J. Phys. **F2** 878 (1972); J. Phys. **C14** 3795 (1981)

[13] Haydock R., *Solid State Physics* (Academic Press) **35**

[14] Mookerjee A., J. Phys. **C6** L205 91973) ,**C6** 1340 (1973)

[15] Kaplan T. and Gray L.J., J. Phys. **C9** L203 (1976); Phys. Rev. **B14** 3462 (1976) ; Phys. Rev. **B15** 3260 (1977)

[16] Razee S.A., Mookerjee A. and Prasad R.P., J. Phys. Condens. Matt **3** 3301 (1991)

[17] Haydock R. and Nex C.M.M., J. Phys. **C17** 4783 (1984) ;J. Phys. **C18** 2235 (1985)

[18] Lucini N.U. and Nex C.M.M., J. Phys. C (Solid State) **20** 3125 (1987)

[19] Ghosh S., Das N. and Mookerjee A., J. Phys. Condens. Matt **48** 10701 (1997)

[20] Ghosh S., Das N., Dasgupta I., Saha-Dasgupta T. and Mookerjee A., Int. J. Mod. Phys B (submitted) (1998)

[21] Heinrich B. and Cochran J.F., Adv. Phys. **42** 523 (1993)

[22] Mookerjee A. and Prasad R., Phys. Rev. **B48** 17724 (1993)

- [23] Gonis A., Turchi P.E.A., Kudronovský J., Drchal V., and Turek I., *J. Phys. Condens Matter* **8** 7869 (1996)
- [24] Razee S.S. and Prasad R., *Phys. Rev. B* **48** 17724 (1993)
- [25] Biswas P.P., Sanyal B., Fakhruddin M., Halder A., Ahmed M. and Mookerjee A., *J. Phys. Condens Matter* **7** 8569 (1995)
- [26] Skriver H.L. and Rosengaard N.M., *Phys. Rev. B* **43** 9538 (1991)
- [27] Saha T. and Mookerjee A., *J. Phys. Condens Matter* **8** 2395 (1996)
- [28] Blügel S., *Lectures in Magnetism on Surfaces*, I.C.T.P., Trieste, (1995)

Figure 1

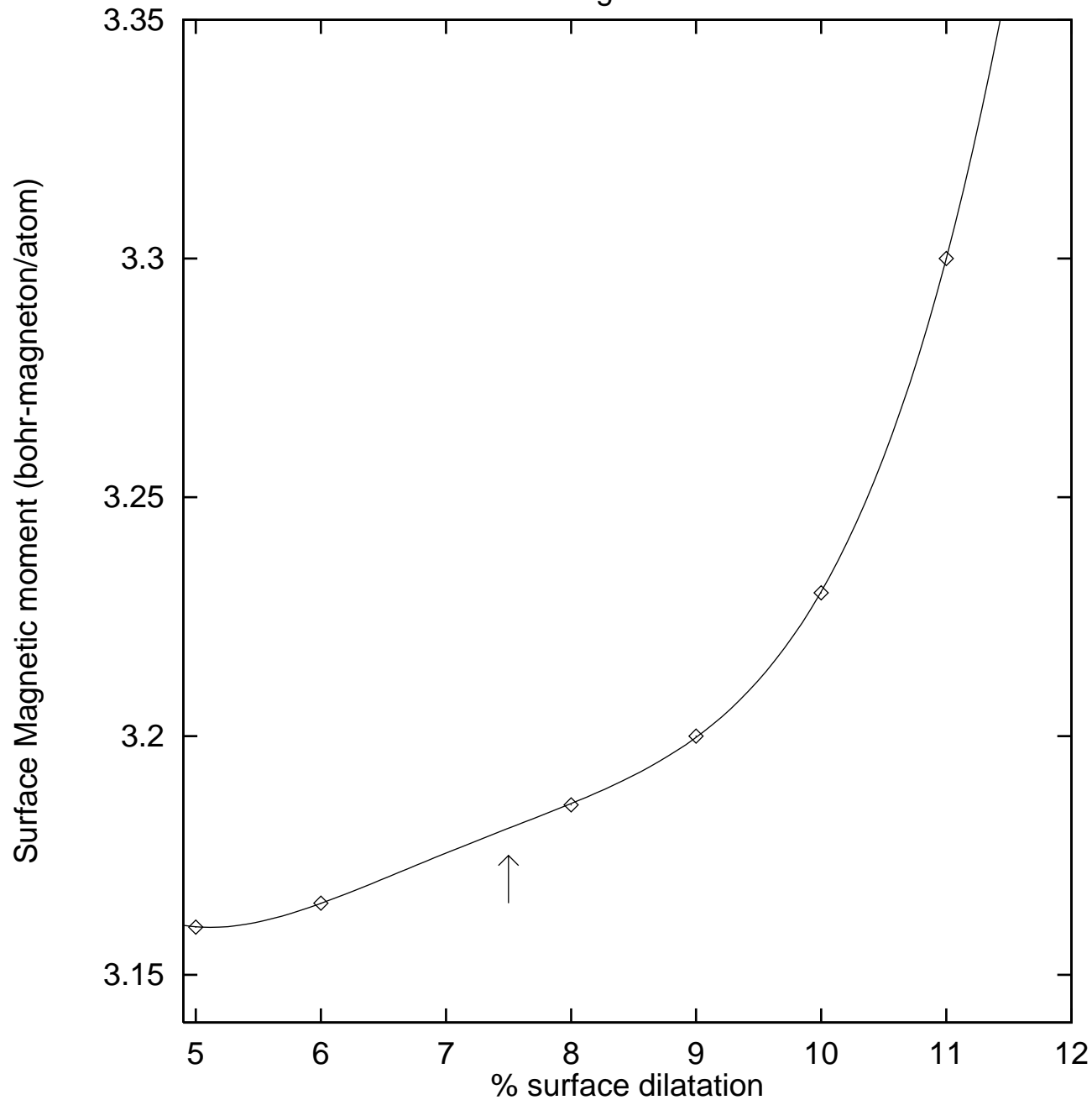


Figure 2(a)

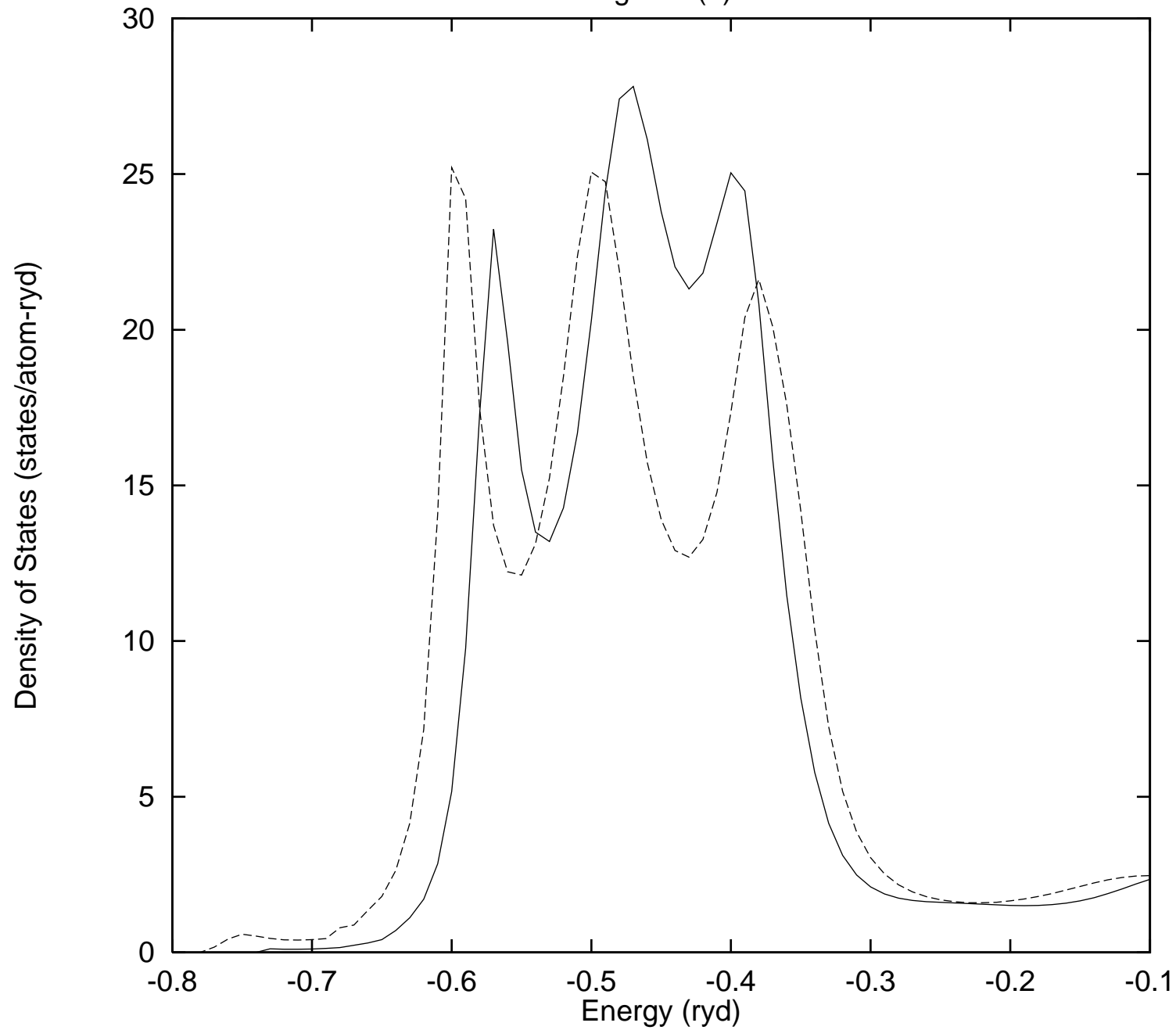


Figure 2(b)

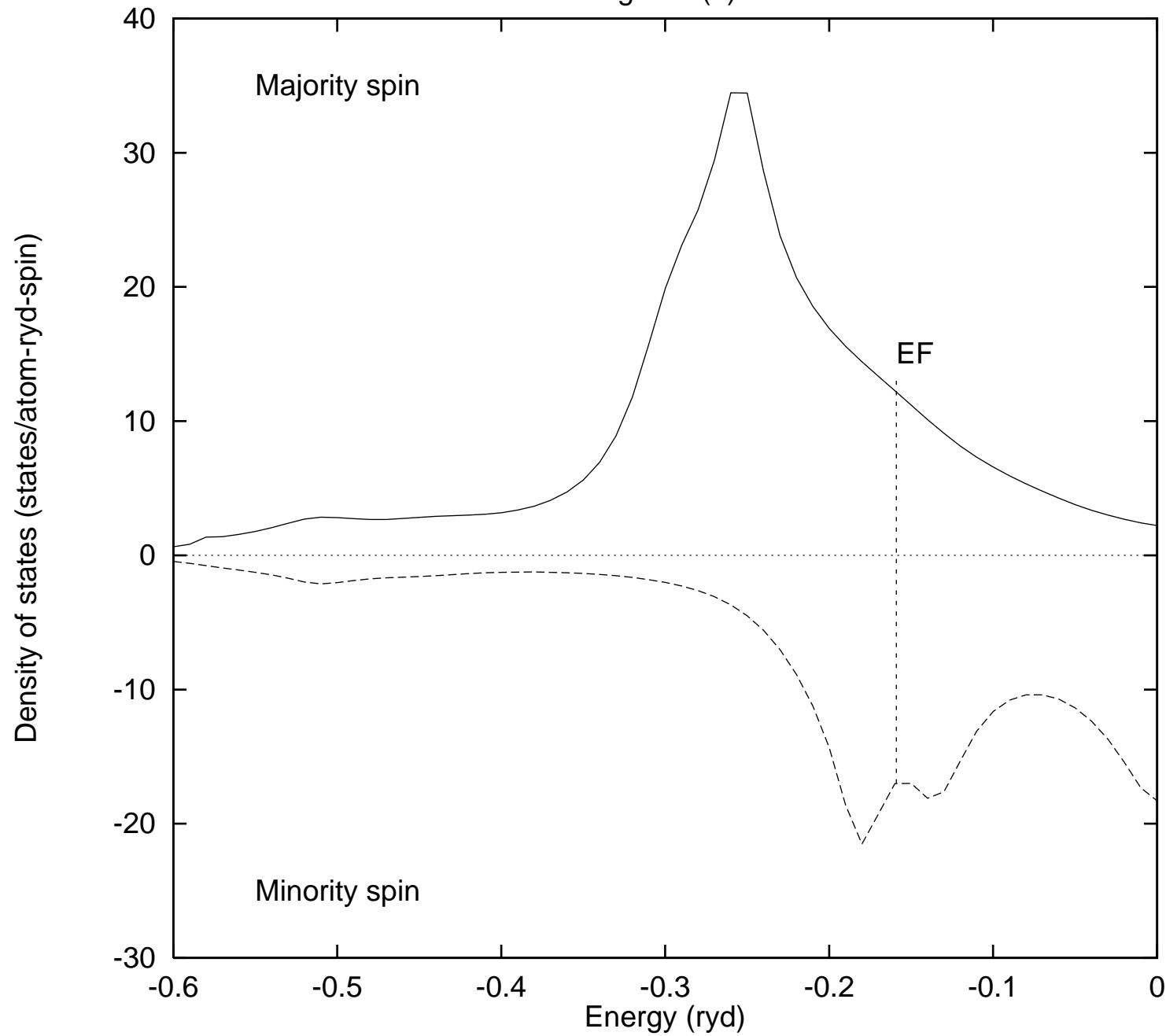


Figure 3

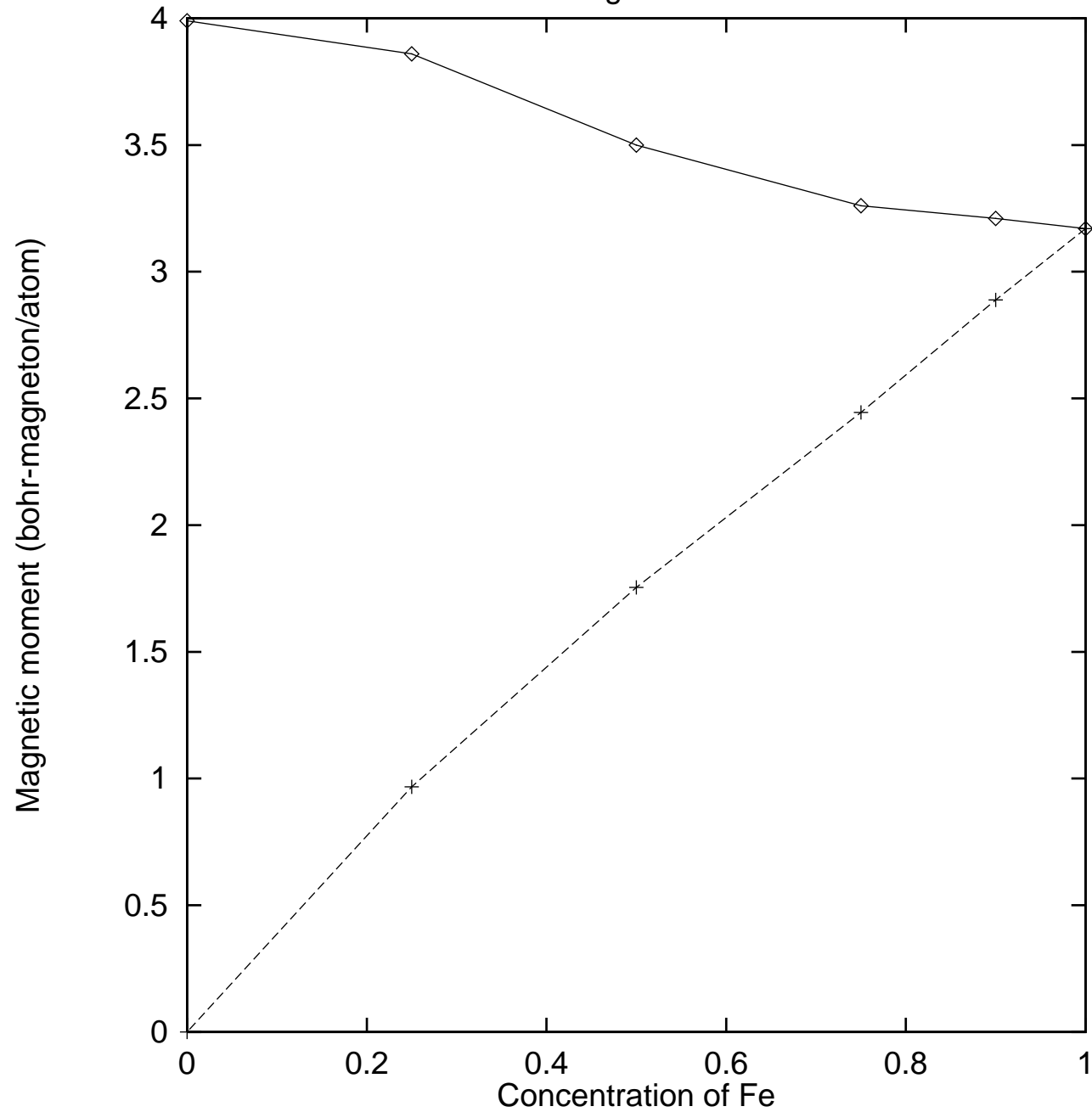


Figure 4

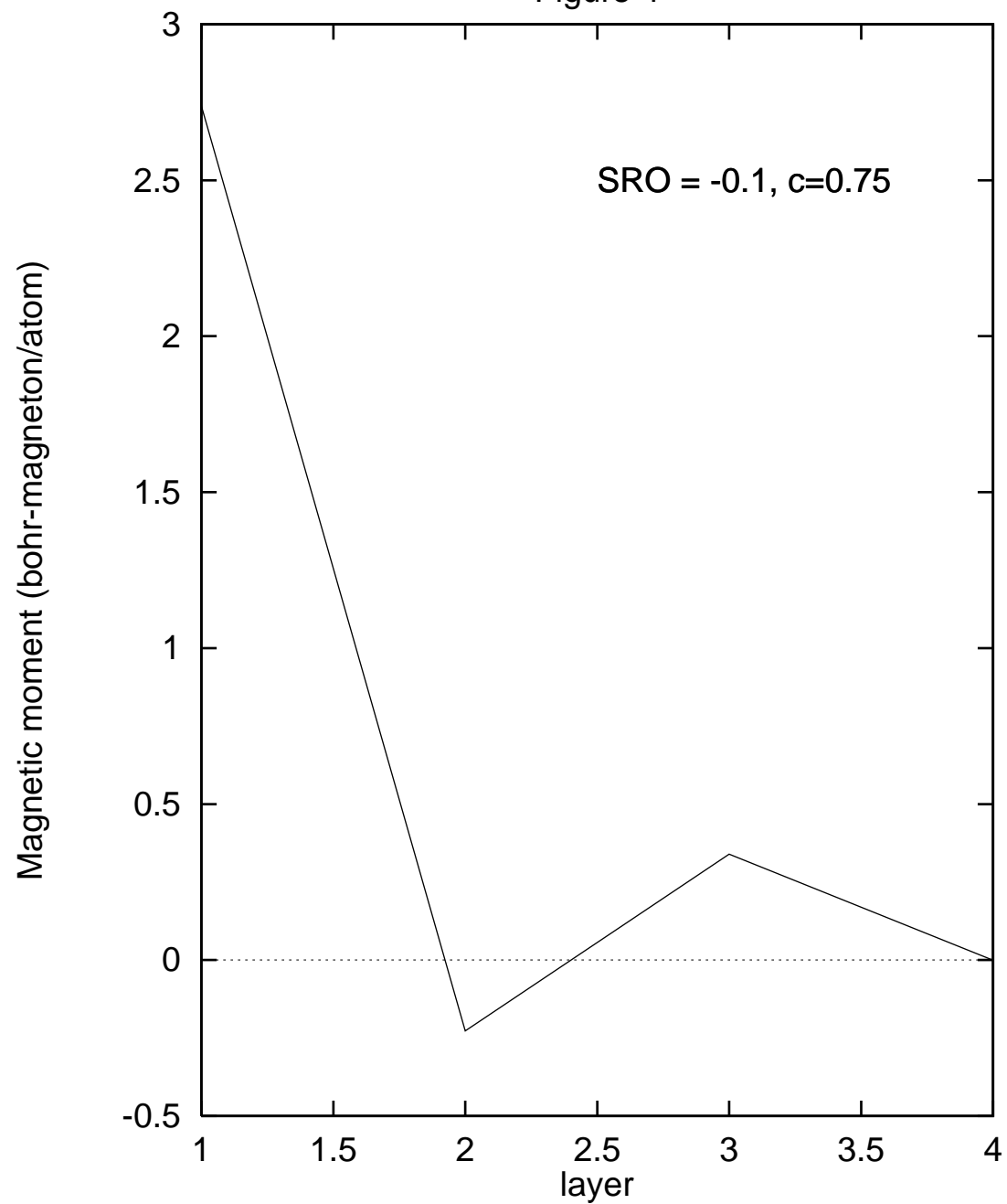


Figure 5

